Design of a hybrid adaptive sunshade with a knitted textile and shape memory alloy

Lanfranco, Valerio; Navarro, Alessandra Luna; Popescu, Mariana

DOI
10.21606/TI-2023/103

Publication date
2023

Document Version
Final published version

Published in
Proceedings of Textile Intersections Conference 2023

Design Research Society DRS
EXTILE INTERSECTIONS
Loughborough University, London
20 - 23 September 2023

Design of a hybrid adaptive sunshade with a knitted textile and shape memory alloy

Lanfranco, Valerio[a]; Navarro, Alessandra Luna[b]; Popescu, Mariana*[a]

[a] Faculty of Civil Engineering and Geosciences, Delft University of Technology, Delft, The Netherlands
[b] Faculty of Architecture and the Build Environment, Delft University of Technology, Delft, The Netherlands
* m.a.popescu@tudelft.nl

The higher complexity of adaptive façades with respect to conventional static façades hinders their applicability to the built environment. To address this, passive solutions aim at lowering the number of components while preserving the benefits of these systems. In this paper the design of a two-component passive dynamic sunshade that combines Shape Memory Alloys (SMAs) and knitted textile is presented. The novelty resides in the way the textile acts as an active member of the system, counteracting the SMA when in its martensitic (inactive) stage. The properties of the textile and design of the systems repeating movement are determined through mechanical testing. With nodal thermal modelling the main drivers of the SMA spring temperature have been studied. Results show that it is possible to achieve a promising range of movement with the proposed system, but both the textile and the spring could be more optimized to achieve a larger stroke. Results of the thermal analysis highlight that there is a need to concentrate the solar radiation on the spring for it to be independent from the outdoor temperature and work solely with solar radiation. Overall, the presented research expands the knowledge on the design of low-components-based passive sunshades and showcases an example of how textile can become an active member of the mechanical system.

Keywords: passive dynamic shading; CNC knitting; shape memory alloy sunshade; adaptive façades

1. Introduction

The building sector is responsible for 40% of the consumed energy and 36% of the greenhouse gas emissions in the European Union (European Commission, 2020). Adaptive façades could be promising candidates to help in the fulfilling of the ambitious Green Deal target of carbon neutrality by 2050 as they reduce the energy demand of buildings during the use stage. In contrast to conventional static façades, adaptive façades can change their performance in response to changes in boundary conditions. (Attia et al., 2018; Voigt et al., 2022). The most effective designs to save energy are sunshades that lower the cooling energy demand by minimizing solar gains (Bui et al., 2020; Al-

DOI: https://doi.org/10.21606/TI-2023/103.

Masrani et al., 2018; Loonen et al., 2013) while increasing user comfort (Luna-Navarro et al., 2023). However, the adoption of adaptive facades is hindered by their higher complexity and cost during the operational phase (Loonen et al., 2013). Generally, adaptability can be achieved through active systems, which require an external stimulus to activate, or passive systems that rely on material behaviour and physical phenomena (Loonen et al., 2013). Passive solutions have an advantage over the active ones due to their operational simplicity with few components and the lack of high-tech electronic components (Böke et al., 2022).

Therefore, adaptive façades could be promising solutions to reduce the energy demand of buildings and increase user comfort. However, they currently require multiple components and extensive maintenance due to complex mechanical operation, which is a barrier to their lifespan. Passive solutions are possible candidates to help reduce the complexity of these systems as they rely on intrinsic material properties. Given the efficiency of dynamic sunshades in lowering the cooling load of buildings, this paper presents the design of a passive system working solely with two components.

2. State of the art

In this work, passive strategies are referred to as those that do not require electricity to activate and that rely on material behavior and physical phenomena such as phase change.

Amongst passive strategies, Phase Change Materials (PCMs) have gained the attention of researchers due to their ability to store latent heat and release it later. (Lelieveld, 2013). Despite many applications in the opaque part of the facade, Goia et al., (2014) and Li et al., (2022) studied their applicability for sunshade designs. The main drawbacks of this technology in sunshade designs are cost (Mohtashami et al., 2022; Li et al., 2022), and uneven release of heat (Goia et al., 2014). Careful control of the transition temperature for the PCM to go through its phase transition is needed (Goia et al., 2014; Li et al., 2022; Waqas & Din, 2013). Moreover, large amounts of material are needed to obtain a satisfactory performance (Waqas & Din, 2013).

Examples of passive sunshade strategies include those leveraging the hygroscopic properties of wood. However, the stimulus (humidity) and the response wanted (lower solar gains) might not be related (El Houda & Mohamed, 2018). Furthermore, the system needs to be investigated in terms of user acceptance as many small openings are introduced in the field of view of the user (Ibrahim et al., 2020).

Thermochromic glazing is another prominent technology as it can reduce solar gains in the summer while allowing them in winter. Furthermore, its transparency allows for continuous view to the outside. However, problems linked to the technology include stability and costs (Fabiani & Pisello, 2021), colour (Ke et al., 2022), toxicity, and difficulty of configuration (Cao et al., 2020).

Due to their ability to work as actuators, Shape Memory Materials are attractive materials for passive sun shading. This family comprises Shape Memory Polymers (SMPs) and Shape Memory Alloys (SMAs). While SMPs are low cost, biocompatible, highly deformable (Fiorito et al., 2016) and easy to produce, they are sensible to UV corrosion (Sun et al., 2012) and hardly reversible due to increased stiffness at low temperatures (Yoon 2019; Yoon & Bae, 2020). SMAs display similar characteristics to SMPs in terms of costs and biocompatibility (Fiorito et al., 2016) but they also are corrosion resistant, and less

deformable (Soother et al., 2020). The difference between SMPs and SMAs resides in how their stiffness changes when activated. While SMPs become softer at higher temperatures, SMAs become stiffer, making them possible candidates as sensors and actuators of sunshade designs. Actuators, in particular, benefit from stiffness as it ensures accurate and controlled mechanical movements, minimizing unwanted deformations or flexing, thus enabling predictable and repeatable motion. SMAs hold the promise to reduce the complexity of mechanical systems by reducing the number of components and minimizing the number of interactions between them. The solutions proposed by researchers for sunshade designs that use this technology comprise foldable structures (Pesenti et al., 2018; Yi et al., 2020), rotating systems (Mansourizadeh et al., 2021; Vercesi et al., 2020), movable louvers (Grinham et al., 2014), moving sails (Kim et al., 2023; Denz et al., 2021), and meshes (Denz, et al., 2021). Despite SMAs' capability of reducing the mechanical complexity of passive systems by acting both as sensors and actuators, current designs are made up of many small components that complicate the mechanical functioning during the operational phase. Furthermore, most of the designs always occlude the occupant's field of view, which may hinder their applicability to real-life scenarios. Finally, every design, apart from ADAPTEX (Denz et al., 2021), makes use of a secondary biasing spring to counteract the SMA, adding more components to the functioning of the system.

Textiles are a versatile material when it comes to sunshade designs, being used in awnings, tensed canopies, roller blinds, and big tensile structures that create large areas of shade. In addition to their ability to create shade, textiles can also store tension, which confers the possibility to use them as an active part in shading systems. Specifically, knitted textiles can stretch considerably and can be tailored to accommodate different features such as channels and inlays easily during fabrication. The ability to store tension, the stretchability, and the customization potential of knitted textile makes them promising in counteracting the SMA in its martensitic state while allowing coverage in its austenitic one.

The system presented in this paper investigates the use of tensioned knitted textiles as a possible candidate to counteract the SMA during its inactive stage. The choice derives from two main principles: a) using the textile as a biasing member for the SMA spring reduces the number of components as the former works both to create shade and to bring the system back to its original state, and b) knitted textiles can stretch considerably, possibly allowing for the system to occupy a very small portion when inactive, leaving the field of view unoccupied.

The system proposed in this work is depicted in figure 1. The SMA spring placed in the middle of the frame serves as a sensor and actuator that brings the textile down when activated. The sun shading textile is now tensioned. When the SMA goes through martensitic transformation, the tension stored in the textile pulls the system back up.

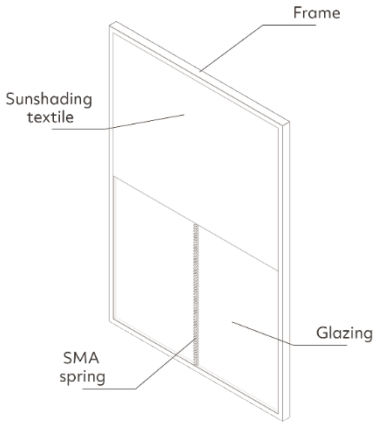

Figure 1. Scheme and components of the system.

3. Methodology

Several aspects ranging from mechanical properties to activation temperature of the SMA are considered in the development of the proposed system. First, benchmarks are set both in terms of thermal comfort for the users and for the mechanical applicability of the system. The former relates to values of solar transmittance of the textile and activation time while the second to the range of movement obtainable such that the system does not interfere with the field of view of the occupants. Following the derived mechanical guidelines, the combined behaviour of the SMA with the textile is investigated. The textile must perform two different actions: stretch to a considerable level (set at 200% to emulate a sunshade that always covers one third of the window, and the full glazing when activated), and have some pullback force that brings the SMA back to its original state.

3.1. Testing Setup

The development comprises an iterative process of producing and testing textile specimens. The performed tests are: simple lateral loading (LL), lateral loading with metal guides (LLG), and with an external elastic (LLEG). A total of 21 CNC knitted specimens are tested by hanging in a testing frame (figure 2.A), adding the eventual metal guide (figure 2.B), and subjecting them to progressive loading (figure 2.C) and unloading while measuring the deformation at each step (figure 2.D). Each measurement serves for the construction of loading and unloading deformation curves to characterize each specimen.

Figure 2. Textile testing setup. A) positioning on the top hooks; B) slide of the metal guide; C) progressive loading and measure of deformation; D) progressive unloading and measurement of residual deformation.

3.2. Textile Development

The textiles are produced on a 10.2-gauge flatbed knitting machine, using a Polyester (PET) yarn and an Elastane and Polyamide (50/50 ratio) yarn. The tested samples combine two main knitting patterns: the alternating bed single jersey, also referred to as "ALT" (figure 3.A), and the double jersey, also referred to as "RIB" (figure 3.B). These patterns are chosen as they exploit the natural curvature given by the knitting process to the textile.

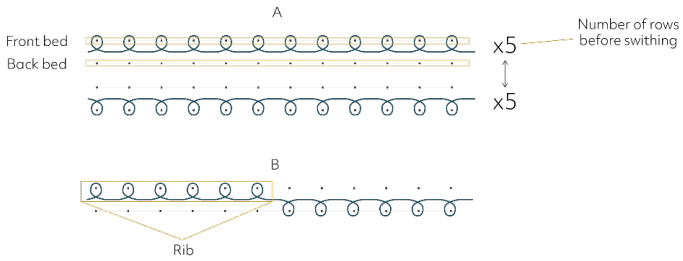

Figure 3. Knit patterns used. A) alternating bed single jersey (ALT); B) double jersey (RIB).

The specimens can be divided into 3 groups (shown in tables 1-3) depending on the type of used yarn (PES, EL, PES with EL inlay). In this work, inlays are referred to as vertical yarns inserted and tensioned in the textile during or after production. The following parameters are explored during production and testing: number of rows knitted on one bed before switching to the opposite bed in the ALT design, number of needles used to create a rib in the RIB design, number of plies, and finally resting length, number, and positioning of inlays. In group 3 (table 3) the inlay is inserted manually after production except for the designs RIB10_PET_1-6 where the elastic inlay is inserted by the CNC knitting machine during production. The desired length of elastic inlay is achieved by tensioning in post-production.

Table 1. Specimens produced using the PES thread. Properties about knit pattern and the loading conditions.

Name	Knit Architecture	N. of plies	Loading condition	Load direction	N. of loops
ALT5_4T	ALT (5 rows before switch)	4 PES	LL, LLEG	Warp	120 (weft) 210 (warp)

ALT10_3T	ALT (10 rows before switch)	3 PES	LL, LLEG	Warp	120 (weft) 210 (warp)
ALT10_4T	ALT (10 rows before switch)	4 PES	LL, LLEG	Warp	120 (weft) 210 (warp)
ALT10_5T	ALT (10 rows before switch)	5 PES	LL, LLEG	Warp	120 (weft) 210 (warp)
ALT10_6T	ALT (10 rows before switch)	6 PES	LL	Warp	120 (weft) 210 (warp)
ALT 15_3T	ALT (15 rows before switch)	3 PES	LL, LLEG	Warp	120 (weft) 210 (warp)

Table 2. Specimens produced using the EL thread. Properties about knit pattern and the loading conditions.

Name	**Knit Architecture (*)**	**N. of plies**	**Loading condition**	**Load direction**	**N. of loops**
ALT10_ET	ALT (10 rows before switch)	1 EL	LL	Warp	60 (weft) 105 (warp)
ALT10_3T_W	ALT (10 rows before switch)	1 EL	LL	Warp	120 (weft) 55 (warp)
ALT10RIB3_ET_W	ALT (10 rows before switching) RIB (3 needles rib)	1 EL	LL	Warp Weft	120 (weft) 55 (warp)
RIB1_ET_W	RIB (1 needle rib, skip 1)	1 EL	LL, LLG	Warp	120 (weft) 55 (warp)
RIB2_ET_W	RIB (1 needle rib, skip 1)	1 EL	LL, LLG	Warp	120 (weft) 55 (warp)

(*) Every ALT design was made by skipping one needle as the elastic yarn was too tight and would get tangled in the machine. In the RIB designs, this was prevented by skipping one or more needles between a rib and the next one.

Table 3. Specimens produced using the PES thread with the EL inlay. Properties regarding the knit pattern with the loading conditions.

Name	**Knit Architecture**	**N. of plies**	**Loading condition**	**Load direction**	**N. of loops**
ALT10_PET_1	ALT (5 rows before switch)	4 PES 10 EL (10.3 cm)	LL	Warp	120 (weft) 210 (warp)
ALT10_PET_2	ALT (10 rows before switch)	4 PES 10 EL (14.2 cm) diag.	LL	Warp	120 (weft) 210 (warp)

ALT10_PET_3	ALT (10 rows before switch)	4 PES 10 EL (14.4 cm) diag.	LL	Warp	120 (weft) 210 (warp)
ALT10_PET_4	ALT (10 rows before switch)	4 PES 10 EL (14.4 cm) diag.	LL	Warp	120 (weft) 210 (warp)
ALT10_PET_5	ALT (10 rows before switch)	4 PES 10 EL (14.4 cm) diag.	LL	Warp	120 (weft) 210 (warp)
RIB10_PET_1	RIB (5 needles)	4 PES 20 EL (12.2 cm)	LL	Weft	100 (weft) 90 (warp)
RIB10_PET_2	RIB (5 needles)	4 PES 16 EL (16.6 cm) diag.	LL	Weft	140 (weft) 180 (warp)
RIB10_PET_3	RIB (5 needles)	4 PES 14 EL (16.6 cm) diag.	LL	Weft	140 (weft) 180 (warp)
RIB10_PET_4	RIB (5 needles)	4 PES 12 EL (16.6 cm) diag.	LL	Weft	140 (weft) 180 (warp)
RIB10_PET_5	RIB (5 needles)	4 PES 10 EL (16.6 cm) diag.	LL	Weft	140 (weft) 180 (warp)

3.3. Spring Design

A simple algorithm is implemented for the design of the SMA spring such that the textile stroke is maximized. An assumption on the modulus of rigidity of the spring is made by testing a spring from a supplier because SMA properties vary greatly depending on the alloy composition, manufacturing parameters, and supplier (Yamauchi et al., 2011). The algorithm takes the tested textile's deformation curves and applies the formula:

$$\delta = 8PD^3n/Gd^4$$

Where:

δ is the deflection [mm]

P is the applied force from the tensioned textile [N]

D is the mean coil diameter [mm]

n is the number of coils [-]

G is the modulus of rigidity [MPa]

d is the wire diameter [mm]

The algorithm also checks that the spring remains in the elastic region, avoiding plastic deformation.

3.4. Drivers of the SMA temperature

As the primary goal of a sunshade is to reduce solar gains, the system efficiency is tested during a typical day. This means analysing the temperature of the SMA spring and the drivers of the latter. To do so, a nodal thermal model is implemented in MatLab. The model first takes environmental data from an EnergyPlus Weather File (EPW) during a summer day in Rotterdam (NL). After specifying the nodes geometry and their properties it constructs the matrix with the involved heat transfer for each node. The script then solves the matrix for each timestep of the simulation considering a timestep of 15 minutes for the 10 hours considered in the simulation. At each timestep the temperature of each node is calculated together with the heat transfers involving the SMA spring. The following assumptions are made in the model: a) spring geometry is assumed to be a cylinder for the calculation of view factors and convective heat transfer coefficients, b) the heat exchange with the window frame is ignored, c) emissivity of the SMA and solar transmittance of the textile are assumed at 0.3, d) the SMA is activated at a specific temperature and not over a span and it does not exhibit hysteresis.

4. Results

In this section the results for each section of the research are presented.

4.1. Textile characterization

Figures 4.A-F present the mechanical characterization of the counterAKT system. The results are graphed in loading (brighter) and unloading (lighter) curves of the textiles during the experiments. The specimens not tested under the LLG conditions were produced without holes for the guide to run through, making them unfeasible to test under this condition. It is important to note that the vertical axis represents the load per each side of the textile and to find the total force the textile was subject to, the force should be multiplied by a factor 2. The point of application of the force did not matter as the textiles had a rigid wooden bar that would distribute the load along the width.

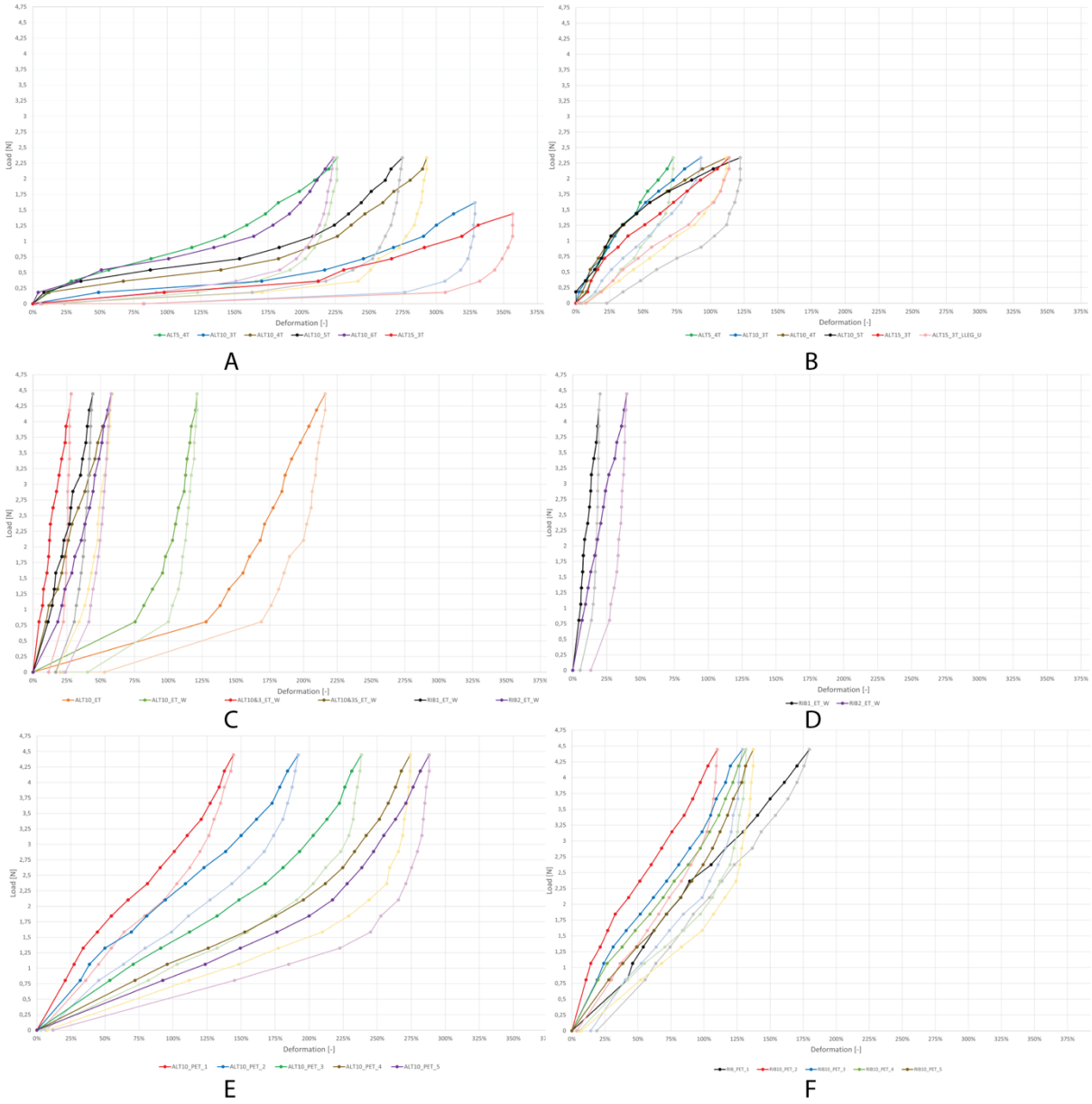

Figure 4. Results from the different tests. A) PES group under LL; b) PES group under LLEG; c) ET group under LL; d) ET group under LLG; e) PES+ET ALT group under LL; f) PES+ET RIB group under LL.

The first experiments concern only the PES textiles with alternating geometry without lateral restriction from the guides. The tests show the largest deformation among the specimens (up to circa 350% for the ALT15_3T) but an inability of the samples to go back to the original shape when partly unloaded. Furthermore, the study of different parameters shows the following trends:

- Adding more plies increases the stiffness of the textile, leading to less deformation for an equivalent load.
- Bigger ribs lead to more deformation for an equivalent load.

The LLEG tests show increased stiffness of the specimens without reducing the gap between the loading and unloading curve. In general, it noted that despite the thread of the specimen being made

of PES, the textile behaves similar to an elastomer in loading and unloading (figures 4.A-B). The difference between the loading and unloading curves in an elastomer is caused by elastic hysteresis whose origin is attributed to the energy dissipated due to the material internal friction (Illinois Tool Works Inc., sd).

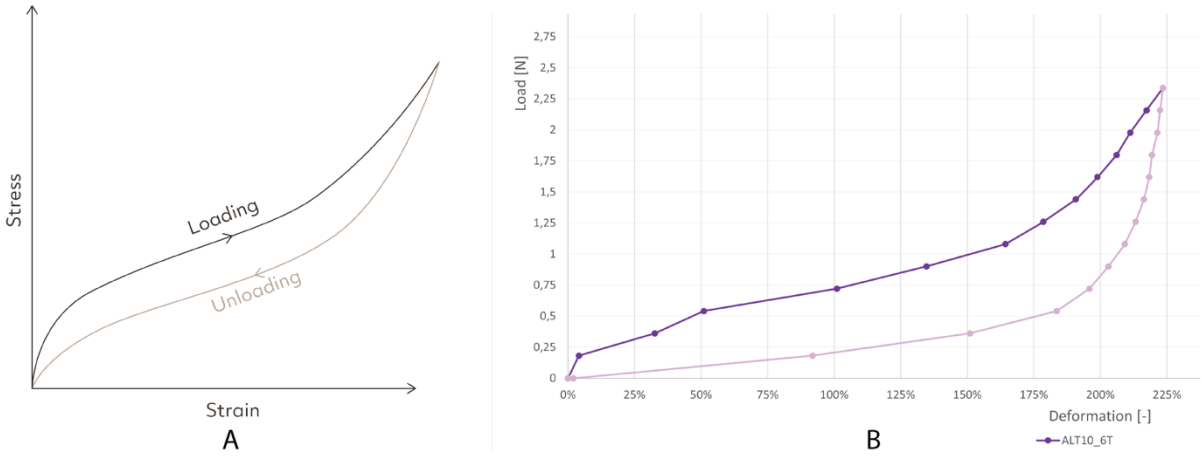

Figure 5. Similarity between the typical elastomer curve (A) and one of the specimens (B) (right image retrieved from: https://www.toppr.com/ask/content/concept/behaviour-of-rubber-and-spring-208795/).

Textiles group 2 shows a stiffer behaviour when compared to the first group. Not much difference is observed between the specimens except for the two ALT10 designs where a large deformation is achieved in the beginning. Furthermore, elastic hysteresis is still observed but more contained with respect to the textile Group 1.

Finally, the performance of textile Group 3 is located between that of the two previously described groups. The PES+EL textiles show a great range of behaviours even though the knit architecture of the PES part is kept uniform throughout the specimens (with the differentiation between the ALT and the RIB design). Therefore, the significant difference between the specimens can be attributed to the EL part where the following trends are observed:

- decreasing the number of elastic inlays leads to more deformation and more elastic hysteresis, making the sample behave similar to the one observed in textile Group 1;
- increasing the elastic inlays length while creating a zig-zag pattern leads to more deformation.

While the specimens in figure 3E are the ones where the inlay was inserted manually, the ones in figure 3F are the ones where the elastic was laid-in during production and post tensioned. Amongst these the RIB10_PET_1 shows the greatest deformation at the expense of a relatively low elastic hysteresis. As a result, this textile is chosen as the reference textile to test for the ideal spring geometry.

4.2. Spring dimensioning

After an optimization consisting of 4810 runs, the ideal spring geometry for the RIB10_PET_1 design has the properties listed in table 4.

Table 4. Ideal spring geometry for RIB_PET_1 design.

Textile specimen	Wire diameter [mm]	Mean coil diameter [mm]	Number of coils [-]	Textile deformation Austenite [-]	Textile deformation Martensite [-]	Total stroke [mm]	Stroke / initial length [-]
RIB10_PET1	2	25.4	30	180%	75%	97	131%

The analytical results show that it is possible to achieve a stroke that is above 100% of the original length of the textile.

4.3. Thermal model

Figures 6A-D show the temperature profiles of the various nodes and the heat transfers related to the SMA spring for an activation temperature of the SMA of 19°C and 20°C.

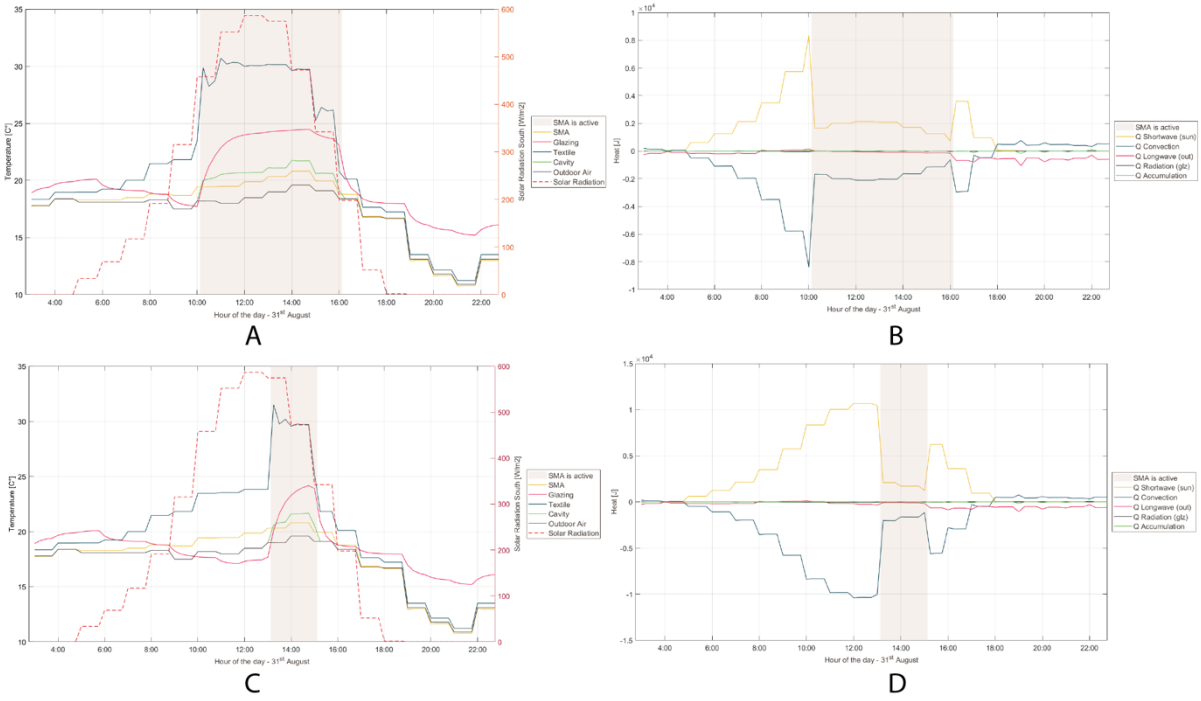

Figure 6. Thermal model results from the MatLab model. A) Temperature profiles when the SMA activation temperature is 19°C; B) Heat transfers when the SMA activation temperature is 19°C; C) Temperature profiles when the SMA activation temperature is 20°C; D) Heat transfers when the SMA activation temperature is 20°C.

In both cases the temperature of the SMA spring is an offset of the outdoor temperature. It is observed that the temperature of the glazing has a delay and does not look like a step function compared to that of the other nodes. Furthermore, the temperature of the glazing increases when the blind is closed. Solar radiation and convection to the outside are the most dominating heat transfers for the SMA. Meanwhile, the longwave radiation heat exchange plays a minimal role during the day and a bigger one during the night. For what concerns the radiation with the glazing and the accumulation the values are negligible (approximately equal to zero).

5. Discussion

In terms of mechanical behaviour, the combination of the PES yarn and the EL yarn in textile Group 3 shows the most promising results both in terms of deformation and in terms of recovery. The reason for this lies in the results from the two previous groups. PES-only textiles show an ability to deform considerably under a progressive load, making them great at covering large areas when tensioned and small ones when resting. Combining this property with the reduced elastic hysteresis from the second group gives the specimen the ability to have enough force to raise the system back to its original shape whilst keeping a large deformation. Furthermore, the LLG test worsens the performance of the textiles as it adds friction between the textile and the metal bar. Overall, elastic hysteresis has been dealt with partly, but varying the parameters of textile Group 3 could lead to better results. Additionally, it is important to note that the two knit architectures explored within this work only cover a small portion of the many customizations that one can achieve with knitting, and even within these two, the parameters changed are limited to a couple of iterations.

The spring obtained through the script is the best in terms of maximizing the stroke, but this result is highly dependent on the capacity of the textile to deform and return to its original state. By having a better performing textile in terms of deformation and elastic hysteresis the achieved stroke could reach the benchmark of 200%. This would mean that the blind would always cover only one third of the window while currently this is about half.

The thermal model shows that the SMA follows the outdoor temperature with an offset attributable to the solar gain. However, the convection with the outside air still plays a major role in determining the actuator's temperature. The glazing reaches a higher temperature when the blind is down due to the loss of the convective heat transfer with the outdoor air. In this case its temperature is mainly driven by the convection with the inside environment which has been set at 24°C. However, this does not play a role in the temperature prediction of the SMA where the heat transfer through radiation with the glazing is always close to zero.

6. Conclusion and outlook

Overall, this paper showcases the process of designing a proof of concept for a low-component, passive dynamic sunshade. CNC knitting proved to be efficient both in producing many specimens to test and in inlaying the elastic in a controlled way. However, the deformations obtained through all the specimens did not reach enough range to achieve the benchmark of 200% when coupled with the SMA spring. Moreover, even though the inlay was inserted during production, it had to be tensioned afterwards manually. The analytical solution to find the best SMA spring geometry produced good results, but the assumed properties of the alloy need to be checked via mechanical testing to be validated. The thermal modelling provided insight on the temperatures reached by the components of the system and showed that the major contributors to the SMA temperature are the solar gain and the convective loss. However, the latter plays a major role as the SMA temperature is just an offset of the outdoor air temperature. Furthermore, the activation temperature of SMAs is highly dependent on their composition and not easily fixed. In the examples shown we observe two very different performances for two similar activation temperatures. To bring a similar system to a full working product further research must be done to optimize its performance. Firstly, the textile needs to have

more iterations in terms of knit pattern and inlay parameters to find more deformable specimens with less elastic hysteresis. Following the logic of textile Group 3 with PES thread and EL inlay seems to give the most promising results. In terms of textile manufacturing there is a need to tension the inlay during production for it to be serialized. Moreover, PES thread is UV resistant, which allows for the sunshade to be sun-exposed without being damaged. The lack of SMAs standardization makes it hard to predict the behaviour of the spring in the system. For now, mechanical testing is still needed to create a fully functioning system. Finally, as the temperature of the SMA is mainly driven by the outdoor air temperature, studies on how to limit the heat loss through convection or how to increase the gain from solar radiation is needed. This would ensure that the system gets triggered when the solar loads exceed a certain design threshold, and that the system would not be triggered by a particularly hot cloudy day. Furthermore, this would help with the unpredictability of the SMA temperature due to its composition, as higher temperature reached by the component would make its behaviour more controllable. Finally, modelling the SMA without accounting for the fact that it transforms over a span of temperature rather than on a specific set temperature is a limit of the study. However, in applications relying on high solar radiation, the simplified approach may still be suitable, as the temperatures reached exceed typical outdoor air temperatures.

References

Al-Masrani, S. M., Al-Obaidi, K. M., Zalin, N. A., & AIda Isma, M. I. (2018). Design optimisation of solar shading systems for tropical office buildings: Challenges and future trends. *Solar Energy*(170), 849-872.

Attia, S., Bilir, S., Safy, T., Struck, C., Loonen, R., & Goia, F. (2018). Current trends and future challenges in the performance assessment. *Energy & Buildings 179*, 165-182.

Böke, J., Denz, P.-R., Suwannapruk, N., & Vongsingha, P. (2022). Active, Passive and Cyber-Physical Adaptive Façade strategies: a Comparative Analysis Through Case Studies. *Journal of Facade Design & Engineering, 10*.

Bui, D.-K., Nguyen, T., Ghazlan, A., Ngo, N.-T., & Ngo, T. (2020). Enhancing building energy efficiency by adaptive façade: A computational optimization approach. *Applied Energy*(265).

Cao, X., Chang, T., Shao, Z., Xu, F., Luo, H., & Jin, P. (2020). Challenges and Opportunities toward Real Application of VO_2-Based Smart Glazing. *Matter*(2), 862-881.

Denz, P.-R., Sauer, C., Waldhör, E., Schneider, M., & Vongsingha, P. (2021). Smart Textile Sun Shading Development of Functional ADAPTEX Prototypes. *Journal of Facade Design and Engineering, 9*(1), 101-116.

El Houda, A. N., & Mohamed, D. (2018). Advanced Building Skins Inspired From Plant Adaptation Strategies to Environmental Stimuli: A Review. Médéa.

European Commission. (2020). *In focus: Energy efficiency in buildings*. Retrieved 11 21, 2022, from https://ec.europa.eu/info/news/focus-energy-efficiency-buildings-2020-lut-17_en

Fabiani, C., & Pisello, A. L. (2021). Passive cooling by means of adaptive cool materials. In W. Publishing (Ed.), *Eco-efficient Materials for Reducing Cooling Needs in Buildings and Construction* (pp. 439-457`).

Fiorito, F., Sauchelli, M., Arroyo, D., Pesenti, M., Imperadori, M., Masera, G., & Ranzi, G. (2016). Shape Morphing Solar Shadings: a review. *Renewable and Sustainable Energy Reviews*(55).

Goia, F., Perino, M., & Serra, V. (2014). Experimental Analysis of the energy performance of a full-scale PCM glazing prototype. *Solar Energy*(100), 217-233.

Grinham, J., Blabolil, R., & Haak, J. (2014). Harvest Shade Screens: Programming material for optimal energy building skins. Los Angeles.

Ibrahim, A., Abdelmohsen, S., Omar, W., & Zayan, A. (2020). Extending the Passive Actuation of Low-Tech Architectural Adaptive Systems by integrating Hygroscopic and Thermal Properties of Wood. *Robotic Tectonics, Automation and Interaction, 2*, 641-650.

Illinois Tool Works Inc. (n.d.). *Elastic Hysteresis*. Retrieved 03 30, 2023, from https://www.instron.com/en/resources/glossary/e/elastic-

hysteresis#:~:text=Elastic%20Hysteresis%20is%20the%20difference,testing%20(loading%20and%20unloading).
Ke, Y., Tan, Y., Feng, C., Chen, C., Lu, Q., Xu, Q., Long, Y. (2022). Tetra-Fish-Inspired aesthetic thermochromic windows toward Energy-Saving buildings. *Applied Energy*(315), 1-9.
Kim, M.-j., Kim, B.-g., Koh, J.-s., & Yi, H. (2023). Flexural biomimetic responsive building facade using a hybrid soft robot actuator and fabric membrane. *Automation in Construction*(145), 1-20`.
Lelieveld, C. M. (2013). *Smart Matherials For The Realization Of An Adaptive Building Component.* Delft.
Li, D., Yang, R., Arıcı, M., Wang, B., Tunçbilek, E., Wu, Y., Ma, Y. (2022). Incorporating phase change materials into glazing units for building applications: Current progress and challenges. *Applied Thermal Engineering*.
Loonen, R., Trčka, M., Cóstola, D., & Hensen, J. (2013). Climate adaptive building shells: State-of-the-art and future challenges. *Renewable and Sustainable Energy Reviews*(25), 483-493.
Luna-Navarro, A., Lori, G., Callewaert, D., & Overend, M. (2023). Semi-automated vs manually controlled dynamic facades: assessment through a field study on multi-domain occupant satisfaction. *Energy & Buildings*(286), 1-16.
Mansourizadeh, K., Golahmadi, A., Paoletti, I. M., & Anishchenko, M. (2021). Design of a passive mechanical system actuated by the nitinol helical springs for shading and sustainable development purposes of the buildings. *Building and Environment*(187), 1-15.
Mohtashami, N., Fuchs, N., Fotopoulou, M., Drosatos, P., Streblow, R., Osterhage, T., & Müller, D. (2022). State of the Art of Technologies in Adaptive Dynamic Building Envelopes (ADBEs). *Energies, 15*.
Pesenti, M., Masera, G., & Fiorito, F. (2018). Exploration of Adaptive Origami Shading Concepts through Integrated Dynamic Simulations. *Architectural Engineering, 24*(4).
Soother, D. K., Daudpoto, J., & Chowdhry, B. S. (2020). Challenges for practical applications of shape memory alloy actuator. *Materials Research Express*(7).
Sun, L., Huang, W., Ding, Z., Zhao, Y., Wang, C., Purnawali, H., & Tang, C. (2012). Stimulus-responsive shape memory materials: A review. *Materials and Design 33*, 577-640.
Vercesi, L., Speroni, A., Mainini, A., & Pli, T. (2020). A Novel Approach to Shape Memory Alloys Applied to Passive Adaptive Shading Systems. *Journal of Facade Design and Engineering, 8*(1), 43-64.
Voigt, M., Roth, D., & Kreimeyer, M. (2022). Main Characteristic of Adaptive Facades. Cavtav.
Waqas, A., & Din, Z. U. (2013). Phase change material (PCM) storage for free cooling of buildings - A review. *Renewable and Sustainable Energy Reviews*(18), 607-625.
Yamauchi, K., Ohkata, I., Tsuchiya, K., & Miyazaki, S. (2011). *Shape Memory and Superelastic Alloys.* Woodhead Publishing.
Yi, H., Kim, D., Kim, Y., Kim, D., Koh, J.-s., & Kim, M.-J. (2020). 3D-printed attachable kinetic shading device with alternate actuation: Use of shape-memory alloy (SMA) for climate-adaptive responsive architecture. *Automation in Construction*(114), 1-20.
Yoon, J. (2019). SMP Prototype Design and Fabrication for Thermo-responsive Facade Elements. *Journal of Facade Design and Engineering, 7*(1), 41-62.
Yoon, J., & Bae, S. (2020). Performance Evaluation and Design of Thermo-Responsive SMP Shading Prototypes. *Sustainability*(12), 1-35.

About the Authors:

Valerio Lanfranco: Valerio is a Building Engineer who recently earned his Master's degree in Building Physics and Technology from TU Delft. With a solid foundation in Civil Engineering and a profound fascination for parametric design, he consistently pushes the boundaries of creativity in his projects.

Alessandra Luna Navarro: Alessandra is Assistant Professor in Façade Design and Engineering at TU Delft and a chartered engineer in Italy and the UK. She has obtained her PhD from the University of Cambridge by researching occupant-centred design and operation of facades.

Mariana Popescu: Dr. Mariana Popescu is Assistant Professor of Digital Fabrication at TU Delft with a strong interest and experience in innovative ways of approaching the fabrication process and use of materials in construction. She obtained her PhD in 2019 from ETH Zurich.

Acknowledgements. The authors would like to thank Dr. Roel Schipper and Gertjan Peters for their constructive feedback during the development of the concept and prototype testing shown in this paper.